Chinese Chemical Letters 34 (2023) 107838

Contents lists available at ScienceDirect

Chinese Chemical Letters

journal homepage: www.elsevier.com/locate/cclet

Simple yet extraordinary: Super-polyhedra-built 3D chalcogenide framework of $Cs_5Ga_9S_{16}$ with excellent infrared nonlinear optical performance

Hong Chen[a,b,1], Mao-Yin Ran[a,c,1], Sheng-Hua Zhou[a,c], Xin-Tao Wu[a,b,c], Hua Lin[a,b,c,*], Qi-Long Zhu[a,b,c,*]

[a] State Key Laboratory of Structural Chemistry, Fujian Institute of Research on the Structure of Matter, Chinese Academy of Sciences (CAS), Fuzhou 350002, China
[b] Fujian Science & Technology Innovation Laboratory for Optoelectronic Information of China, Fuzhou 350108, China
[c] University of Chinese Academy of Sciences, Beijing 100049, China

ARTICLE INFO

Article history:
Received 25 July 2022
Revised 29 August 2022
Accepted 20 September 2022
Available online 23 September 2022

Keywords:
Chalcogenide
IR nonlinear optic
Super-polyhedra-built framework
Wide energy gap
Structure-activity relationship

ABSTRACT

Non-centrosymmetric chalcogenides are attracting considerable attention as highly promising infrared nonlinear optical (IR-NLO) candidates, but it is challenging to simultaneously achieve sufficient second-harmonic-generation coefficient (d_{eff} > 0.5 × $AgGaS_2$) and large energy gap (E_g > 3.5 eV). In this work, a novel ternary chalcogenide, $Cs_5Ga_9S_{16}$ with an ultra-wide E_g of 4.05 eV, has been successfully obtained. This sulfide belongs to the monoclinic space group *Pn* (No. 7) with a novel 3D anionic $[Ga_9S_{16}]^{5-}$ framework that is formed by super-polyhedral $[Ga_9S_{23}]$ units through corner-sharing S atoms. Such a unique crystal structure displays desirable characteristics which indicate a promising IR-NLO candidate: favourable phase-matching feature, sufficient d_{eff} (0.7 × $AgGaS_2$), ultrahigh laser-induced damage threshold (31.6 × $AgGaS_2$) and broad transparent region (0.27–14.96 μm). In addition, systematic theoretical studies and structural analysis suggest that the desirable IR-NLO performances can be attributed to the super-polyhedral building blocks. This finding may provide useful insight into the understanding and designing other high-performance IR-NLO candidates with super-polyhedral-built structures.

As the core parts in laser frequency conversion technology, nonlinear optical (NLO) materials have attracted considerable attention because of their capabilities of producing new coherent and tuneable laser source in various ranges [1–5]. To date, the commercially available NLO crystals in IR region are merely ternary chalcopyrite-type $AgGaS_2$ [7], $AgGaSe_2$ [6] and $ZnGeP_2$ [8]. All of them possess sufficient second-harmonic-generation (SHG) coefficient (d_{eff}) but exhibit several intrinsic problems, such as unfavorable laser-induced damage threshold (LIDT) or unexpected multi-photon absorption caused by small energy gaps (E_g), which seriously hindering their further application in the high-power laser bands. Among all the key conditions for an ideal IR-NLO candidate, achieving concurrently strong d_{eff} and wide E_g is the most challenging due to the plausible incompatibility [9,10]. Consequently, developing new IR-NLO crystals with improved comprehensive performance are critically needed and of great significance.

Metal chalcogenides with non-centrosymmetric (NCS) crystal structure is known to be the richest source of promising IR-NLO candidates [11–26]. A large number of new IR-NLO materials have been obtained in recent years, but only a few phase-matching (PM) metal chalcogenides that are able to display strong d_{eff} (> 0.5 × $AgGaS_2$) and large E_g (> 3.5 eV) simultaneously, such as $[Li_2Cs_2Cl][Ga_3S_6]$ (d_{eff} = 0.7 × $AgGaS_2$, E_g = 4.17 eV) [27], $Li_4MgGe_2S_7$ (d_{eff} = 0.7 × $AgGaS_2$, E_g = 4.12 eV) [28], α-Li_2ZnGeS_4 (d_{eff} = 4.7 × $AgGaS_2$, E_g = 4.07 eV) [29], $Cs_2Cd_2Ga_8S_{15}$ (d_{eff} = 0.5 × $AgGaS_2$, E_g = 3.98 eV) [30], $[Ba_4Cl_2][ZnGa_4S_{10}]$ (d_{eff} = 1.1 × $AgGaS_2$, E_g = 3.85 eV) [31], Li_2CdSiS_4 (d_{eff} = 1.0 × $AgGaS_2$, E_g = 3.76 eV) [32], $BaLi_2GeS_4$ (d_{eff} = 0.5 × $AgGaS_2$, E_g = 3.66 eV) [33], $SrZnGeS_4$ (d_{eff} = 0.9 × $AgGaS_2$, E_g = 3.63 eV) [34], $Sr_2CdGe_2OS_6$ (d_{eff} = 0.8 × $AgGaS_2$, E_g = 3.62 eV) [35]. However, the aforementioned compounds are concentrated in complex quaternary or more systems, while simple systems such as ternary compounds are very rare. As far as we know, the existing example is limited to only $BaGa_4S_7$ (d_{eff} = 0.9 × $AgGaS_2$, E_g = 3.54 eV) [36].

In this work, we focus on the ternary A(AE)/M/S (A = alkali metals; AE = alkaline-earth metals; M = group IIIA metal Ga, In or

* Corresponding authors.
E-mail addresses: linhua@fjirsm.ac.cn (H. Lin), qlzhu@fjirsm.ac.cn (Q.-L. Zhu).
[1] These authors contributed equally to this work.

https://doi.org/10.1016/j.cclet.2022.107838
1001-8417/

group IVA metal Si, Ge) system. The [MS_4] tetrahedra are the most common NLO-active units in excellent IR-NLO chalcogenides. Meanwhile, the incorporation of highly electropositive A/AE metals in this system may have the additional advantage of increasing the E_g, which may help to enlarge the LIDT once a NCS material is found. Our systematic exploratory efforts have led to the discovery of a new member with 3D framework structure in this family [37–41], namely, $Cs_5Ga_9S_{16}$. Notably, it shows impressive IR-NLO properties, such as remarkable d_{eff} ($0.7 \times AgGaS_2$), and the largest E_g (4.05 eV) among known ternary NCS chalcogenides. These findings are quite encouraging for an excellent IR-NLO candidate ($d_{eff} > 0.5 \times AgGaS_2$ and $E_g > 3.5$ eV).

The sulfide $Cs_5Ga_9S_{16}$ is a new ternary phase found within the A–M–Q (A = alkali metals; M = group IIIA metal; Q = S, Se, Te) systems. It was obtained through high-temperature solid-phase method with CsCl as flux (detailed synthesis method can be found in Supporting information). The pure phase of the polycrystalline sample was verified based on the powder X-ray diffraction (XRD) results (Fig. S1 in Supporting information). Moreover, TG-DSC studies reveal that $Cs_5Ga_9S_{16}$ can be stable up to 1273 K without any obvious endo- or exo-thermal peaks and weight loss (Fig. S2 in Supporting information). Single-crystal XRD suggests that $Cs_5Ga_9S_{16}$ belongs to the monoclinic space group *Pn* (No. 7), with $a = 9.467(3)$ Å, $b = 9.719(3)$ Å, $c = 18.835(6)$ Å, $V = 1704.3(9)$ Å^3, $Z = 2$ (Table S1), and features a 3D $[Ga_9S_{16}]^{5-}$ framework with the charge balancing Cs^+ ions residing between these voids (Fig. 1). In the structure, 9 crystallographically unique Ga atoms exhibit one type of coordination environment, *i.e.*, the [GaS_4] tetrahedral (Table S2 in Supporting information). The fundamental building block (FBB) is super-polyhedral [Ga_9S_{23}] cluster which is composed of the vertex-sharing S atoms (Fig. 1a). These FBBs are further interlinked with each other *via* sharing S atoms (*i.e.*, S2, S5, S6 and S12) along the three axial positions to form a 3D framework with Cs^+ cations located in the cavities (Fig. 1b). As listed in Table S3 (Supporting information), the Ga atoms exhibit normal Ga–S bond length, ranging from 2.219(4) Å to 2.483(5) Å [42–45]. There are 5 crystallographically unique Cs atomic positions with four various coordination geometries, *i.e.*, bi-capped trigonal prism (CN = 8 for Cs1 and Cs2, $d_{(Cs-S)} = 3.415(4)$–$4.038(4)$ Å), distorted quadrangular

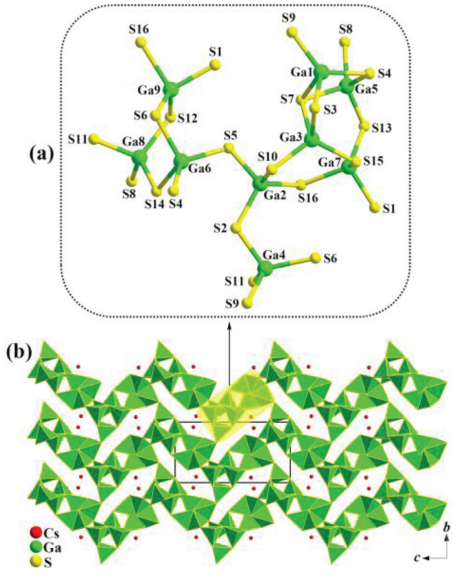

Fig. 1. Illustration of the structure of $Cs_5Ga_9S_{16}$: (a) Coordination geometry of super-polyhedral [Ga_9S_{23}] FBB with the atom number outlined. (b) 3D framework structure of $Cs_5Ga_9S_{16}$ viewed along the *a* direction with the unit cell marked (super-polyhedral [Ga_9S_{23}] cluster is outlined by a dashed area).

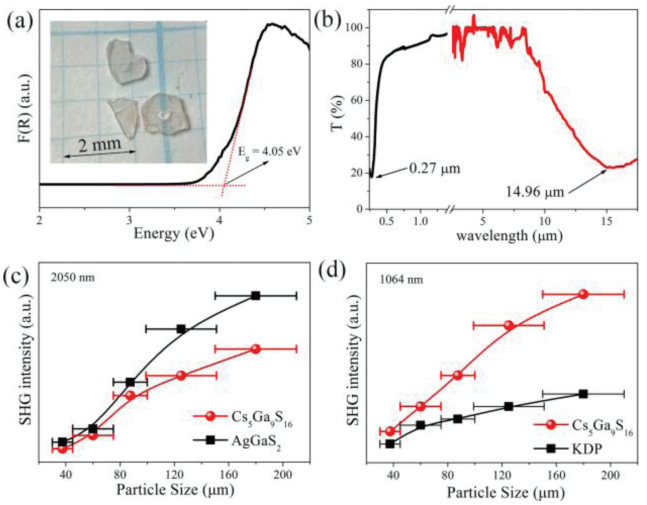

Fig. 2. Experimental results of $Cs_5Ga_9S_{16}$: (a) UV−visible−NIR diffuse reflectance spectrum (inset: polished single crystal wafers). (b) Optical transmisission from UV−vis to IR band. (c, d) SHG signals versus particle size under 2050 nm and 1064 nm Q-switch laser, respectively.

(CN = 10 for Cs3, $d_{(Cs-S)} = 3.398(4)$–$3.998(4)$ Å), mono-capped trigonal prism (CN = 7 for Cs4, $d_{(Cs-S)} = 3.562(5)$–$3.860(4)$ Å), and tricapped trigonal prism (CN = 9 for Cs5, $d_{(Cs-S)} = 3.495(4)$–$3.952(5)$ Å) (Fig. S3 in Supporting information). To the best of our knowledge, such diverse coordination modes of Cs atoms have been coexisted in $Cs_5Ga_9S_{16}$ together is unprecedented in Cs-based chalcogenides.

The UV−visible−NIR diffuse reflectance spectrum of $Cs_5Ga_9S_{16}$ displays one of the widest E_g (*i.e.*, 4.05 eV) among all IR-NLO chalcogenides (Fig. 2a). Such ultra-wide E_g can effectively avoid multi-photon absorptions at the different laser wavelengths, which can obtain a higher LIDT. Moreover, single crystal of $Cs_5Ga_9S_{16}$ with a typical size of 1.5×1.0 mm polished down to ~0.1 mm thickness for the optical transmittance spectra. As given in Fig. 2b, $Cs_5Ga_9S_{16}$ displays a wide optical transmission from the UV−vis (cut-off wavelength: 0.27 μm) to far-IR band (cut-off wavelength: 14.96 μm). The SHG capability of $Cs_5Ga_9S_{16}$ was evaluated through the Kurtz-Perry method [46] using 2050 and 1064 nm laser irradiation, respectively, with the famous IR-NLO crystal $AgGaS_2$ and UV-NLO crystal KDP used for reference. As shown in Figs. 2c and d, the SHG signal tends to attain saturation with the increase of crystal size of sample, which indicates that $Cs_5Ga_9S_{16}$ possesses PM features and exhibits sufficient d_{eff} of about $0.7 \times AgGaS_2$ at 2050 nm and $2.2 \times$ KDP at 1064 nm, respectively. Furthermore, the powder LIDT as another significant parameter for NLO materials was evaluated by single pulse test method at 1064 nm [47]. Consequently, the experimental results of $Cs_5Ga_9S_{16}$ (ca. 89.1 MW/cm^2) is about 31.6 time that of reference $AgGaS_2$ (*ca.* 2.82 MW/cm^2) [48–50] and about 2.2 time that of reference KDP (*ca.* 39.8 MW/cm^2) [51–53], respectively.

To further investigate the microscopic mechanism of the linear optical and NLO properties of $Cs_5Ga_9S_{16}$, first-principles calculations were studied. As displayed in Fig. 3a, the calculated band structure reveals that $Cs_5Ga_9S_{16}$ is an indirect E_g compound with the top of the valence band (VB) and the bottom of the conduction band (CB) occupied the different k-point of the G and F, respectively. As anticipated, the calculated value ($E_g = 2.7$ eV) is underestimated compared to the experimental value ($E_g = 4.05$ eV), due to the own defects of the exchange-correlation function [54–56]. To obtain an accurate optical E_g, the calculated E_g *via* the HSE06 method (4.01 eV) was performed [57,58], which is very close to

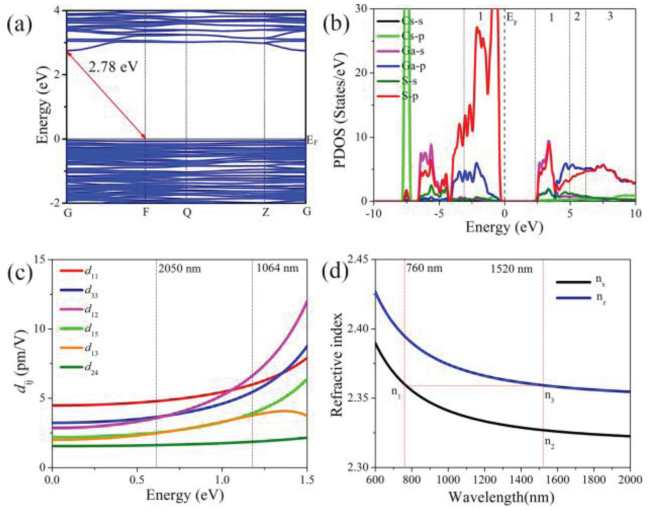

Fig. 3. Theoretical calculation results of $Cs_5Ga_9S_{16}$: (a) Electronic band structure; (b) PDOS (the Fermi level (E_F) is set at 0.0 eV); (c) Frequency-dependent SHG coefficients (d_{ij}); (d) The calculated dispersion of the refractive indices and the shortest type-I PM cut-off wavelength.

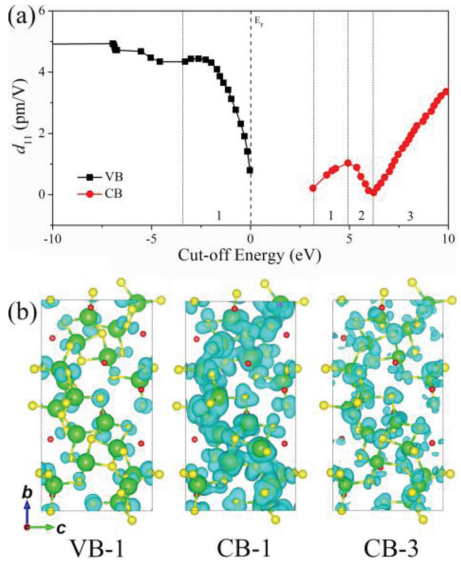

Fig. 4. Theoretical analysis of the NLO source: (a) Cut-off-energy-dependent variation of static coefficient d_{11}; (b) Charge density maps in the VB-1, CB-1 and CB-3 regions along the *bc* plane.

the experimental result. In addition, the first Brillouin zone with high symmetry points of $Cs_5Ga_9S_{16}$ is shown in Fig. S5 (Supporting information). The calculated partial densities of states (PDOS) reveal that the Ga-4p and S-3p, states make the main contributions to the lowest of the CB, while the highest of the VB primarily originates from Ga-4s and S-3p states, indicating that the optical E_g of $Cs_5Ga_9S_{16}$ is mainly due to the 3D $[Ga_9S_{16}]^{5-}$ framework (Fig. 3b). In addition, the SHG coefficients (d_{ij}) of $Cs_5Ga_9S_{16}$ have been also calculated. Based upon the crystal spatial symmetry and the Kleinman restriction [59], there are 6 independent nonzero d_{ij}, *i.e.*, d_{11}, d_{12}, d_{13}, d_{15}, d_{24} and d_{36}, respectively (Fig. 3c). Among them, the effective SHG coefficient d_{eff} at 2050 nm and 1064 nm are about $0.3 \times AgGaS_2$ and $3.9 \times$ KDP, respectively, which is comparable with the experimental results (Figs. 2c and d). Moreover, the minimum phase matching cut-off wavelength were calculated using the equation $n_x(2\omega) = n_z(\omega)$. The calculated PM range of the SHG response for $Cs_5Ga_9S_{16}$ is 760 nm (Fig. 3d) based on the dispersion curves of refractive indices.

The contributions to the principal source of the SHG response from the constituent units were also investigated based on the length-gage formalism technique [60,61]. As displayed in Fig. 4a, it is clear that in the energy regions of VB-1 (−3.0–0.0 eV), CB-1 (3.0–5.0 eV) and CB-3 (6.2–10.0 eV), the d_{11} values increased most notably as the cut-off energy increased, which contribute mainly to the SHG effect. In other words, the states in the VB-1 section (*i.e.*, the Ga-4p and S-3p states) and those in the CB-1 and CB-3 sections (*i.e.*, the Ga-3s, Ga-4p and S-3p states together with minor S-3s) are mainly responsible for the d_{11} (Fig. 4b). These results mean that super-polyhedral $[Ga_9S_{23}]$ cluster in 3D $[Ga_9S_{16}]^{5-}$ framework, contribute to the SHG effect.

In summary, a novel ternary sulfide, $Cs_5Ga_9S_{16}$, is successfully prepared by a facile solid-state method. It adopts a NCS structure featuring a 3D anionic framework formed by vertex-sharing $[Ga_9S_{23}]$ super-polyhedral FBBs, with the intervening spaces filled by charge-balanced Cs^+ cations. Significantly, $Cs_5Ga_9S_{16}$ exhibits excellent IR-NLO performances, such as a favorable PM d_{eff} (0.7-fold that of the benchmark $AgGaS_2$), a large LIDTs (31.6-fold that of $AgGaS_2$), a wide transparent regions (0.27−14.96 μm) and the highest E_g (4.05 eV) at known ternary NCS chalcogenides. Moreover, systematic theoretical analysis indicates that the IR-NLO properties of $Cs_5Ga_9S_{16}$ mainly originate from the contributions of 3D $[Ga_9S_{16}]^{5-}$ framework composed of super-polyhedral $[Ga_9S_{23}]$ groups. This finding further extends the study of promising IR-NLO candidates into the simple ternary system and will promote the development of new NCS chalcogenides with wide energy gaps.

Declaration of competing interest

The authors declare that they have no known competing financial interests or personal relationships that could have appeared to influence the work reported in this paper.

Acknowledgments

This work was supported by the National Natural Science Foundation of China (Nos. 22175175, 21771179 and 21901246), Fujian Science & Technology Innovation Laboratory for Optoelectronic Information of China (No. 2021ZR118), the Natural Science Foundation of Fujian Province (No. 2019J01133) and the Youth Innovation Promotion Association CAS (No. 2022303). The authors thank Prof. Bing-Xuan Li at FJIRSM for helping with the NLO measurements and Prof. Yong-Fan Zhang at Fuzhou University for helping with the DFT calculations.

Supplementary materials

Supplementary material associated with this article can be found, in the online version, at doi:10.1016/j.cclet.2022.107838.

References

[1] F.J. Duarte, Tunable Laser Applications, Chapters 2, 9 and 12, CRC Press, Boca Raton, FL, 2008.
[2] V. Petrov, Prog. Quantum Electron. 44 (2015) 1–106.
[3] V.A. Serebryakov, E.V. Boiko, N.N. Petrishchev, et al., J. Opt. Technol. 77 (2010) 6–17.
[4] X.T. Wu, L. Chen, Struct. Bond. (Berlin, Ger.) 145 (2012) 1–42.
[5] N.L.B. Sayson, T. Bi, V. Ng, et al., Nat. Photonics 13 (2019) 701–706.
[6] A. Harasaki, K.J. Kato, Appl. Phys. 36 (1997) 700–703.
[7] G.C. Catella, L.R. Shiozawa, J.R. Hietanen, et al., Appl. Opt. 32 (1993) 3948–3951.
[8] G.D. Boyd, E. Buehler, F.G. Storz, Appl. Phys. Lett. 18 (1971) 301–304.
[9] H. Chen, W.B. Wei, H. Lin, et al., Coord. Chem. Rev. 448 (2021) 214154.
[10] K. Wu, S.L. Pan, Coord. Chem. Rev. 377 (2018) 191–208.
[11] I. Chung, M.G. Kanatzidis, Chem. Mater. 26 (2013) 849–869.
[12] H. Lin, L. Chen, L.J. Zhou, et al., J. Am. Chem. Soc. 135 (2013) 12914–12921.
[13] L. Kang, M.L. Zhou, J.Y. Yao, et al., J. Am. Chem. Soc. 137 (2015) 13049–13059.
[14] H. Lin, Y.Y. Li, M.Y. Li, et al., J. Mater. Chem. C 7 (2019) 4638–4643.

[15] S.P. Guo, Y. Chi, G.C. Guo, Coord. Chem. Rev. 335 (2017) 44–57.
[16] P.F. Gong, F. Liang, L. Kang, et al., Coord. Chem. Rev. 380 (2019) 83–102.
[17] M.Y. Li, Z.J. Ma, B.X. Li, et al., Chem. Mater. 32 (2020) 4331–4433.
[18] M.Y. Ran, Z. Ma, H. Chen, et al., Chem. Mater. 32 (2020) 5890–5896.
[19] L. Gao, J.B. Huang, S.R. Guo, et al., Coord. Chem. Rev. 421 (2020) 213379.
[20] W.K. Wang, D.J. Mei, F. Liang, et al., Coord. Chem. Rev. 421 (2020) 213444.
[21] H. Lin, W.B. Wei, H. Chen, et al., Coord. Chem. Rev. 406 (2020) 213150.
[22] D. Mei, W. Cao, N. Wang, et al., Mater. Horiz. 8 (2021) 2330.
[23] W. Wang, D. Mei, S. Wen, et al., Chin. Chem. Lett. 33 (2022) 2301–2315.
[24] F. Hou, D. Mei, Y. Zhang, et al., J. Alloys Compd. 904 (2022) 163944.
[25] M.M. Chen, S.H. Zhou, W.B. Wei, et al., ACS Mater. Lett. 4 (2022) 1264–1269.
[26] H. Chen, M.Y. Ran, W.B. Wei, et al., Coord. Chem. Rev. 470 (2022) 214706.
[27] B.W. Liu, X.M. Jiang, B.X. Li, et al., Angew. Chem. Int. Ed. 132 (2020) 4886–4889.
[28] A. Abudurusuli, J.B. Huang, P. Wang, et al., Angew. Chem. Int. Ed. 60 (2021) 24131–24136.
[29] J.H. Zhang, D.J. Clark, J.A. Brant, et al., Chem. Mater. 32 (2020) 8947–8955.
[30] L.Q. Yang, X.M. Jiang, S.M. Pei, et al., ACS. Appl. Mater. Interfaces 14 (2022) 4352.
[31] H. Chen, Y.Y. Li, B.X. Li, et al., Chem. Mater. 32 (2020) 8012.
[32] J.H. Zhang, D.J. Clark, J.A. Brant, et al., Chem. Mater. 32 (2020) 8947.
[33] K. Wu, B.B. Zhang, Z.H. Yang, et al., J. Am. Chem. Soc. 139 (2017) 14885.
[34] Q.Q. Liu, X. Liu, L.M. Wu, et al., Angew. Chem. Int. Ed. 61 (2022) e202205587.
[35] M.Y. Ran, S.H. Zhou, B. Li, et al., Chem. Mater. 34 (2022) 3853–3861.
[36] X.S. Lin, G. Zhang, N. Ye, et al., Cryst. Growth Des. 9 (2009) 1186.
[37] V.V. Atuchin, F. Liang, S. Grazhdannikov, et al., RSC Adv. 8 (2018) 9946–9955.
[38] S.F. Li, X.M. Jiang, B.W. Liu, et al., Chem. Mater. 29 (2017) 1796–1804.
[39] M.Y. Ran, Z. Ma, X.T. Wu, et al., Inorg. Chem. Front. 8 (2021) 4838–4845.
[40] M.M. Chen, S.H. Zhou, W. Wei, et al., Inorg. Chem. 60 (2021) 10038–10046.
[41] W.F. Chen, X.M. Jiang, S.M. Pei, et al., Sci. China. Mater. 66 (2023) 740–747.
[42] H. Lin, L. Chen, J.S. Yu, et al., Chem. Mater. 29 (2017) 499–503.
[43] M.Y. Li, B.X. Li, H. Lin, et al., Chem. Mater. 31 (2019) 6268–6275.
[44] M.M. Chen, S.H. Zhou, W.B. Wei, et al., Adv. Opt. Mater. 10 (2022) 202102123.
[45] Y.Y. Li, W.J. Wang, H. Wang, et al., Cryst. Grow. Des. 19 (2019) 4172–4192.
[46] S.K. Kurtz, T.T. Perry, J. Appl. Phys. 39 (1968) 3798–3813.
[47] M.J. Zhang, X.M. Jiang, L.J. Zhou, et al., J. Mater. Chem. C 1 (2013) 4754–4760.
[48] M.M. Chen, Z. Ma, B.X. Li, et al., J. Mater. Chem. C 9 (2021) 1156–1163.
[49] C. Liu, S.H. Zhou, Y. Xiao, et al., J. Mater. Chem. C 9 (2021) 15407–15414.
[50] Y. Xiao, M.M. Chen, Y.Y. Shen, et al., Inorg. Chem. Front. 8 (2021) 2835–2843.
[51] Y.X. Zhang, B.X. Li, H. Lin, et al., J. Mater. Chem. C 7 (2019) 6217–6221.
[52] H.D. Yang, M.Y. Ran, S.H. Zhou, et al., Chem. Sci. 13 (2022) 10725–10733.
[53] Y.F. Shi, Z. Ma, B.X. Li, et al., Mater. Chem. Front. 6 (2022) 3054–3061.
[54] K.J. Burke, Chem. Phys. 136 (2012) 150901.
[55] N.E. Christensen, A. Svane, E.L. Peltzery Blancá , Phys. Rev. B: Condens. Matter Mater. Phys. 72 (2005) 014109.
[56] K. Govaerts, R. Saniz, B. Partoens, et al., Phys. Rev. B: Condens. Matter Mater. Phys. 87 (2013) 235210.
[57] J. Heyd, G.E. Scuseria, M. Ernzerhof, J. Chem. Phys. 118 (2003) 8207.
[58] F. Ge, B.H. Li, P. Cheng, et al., Angew. Chem. Int. Ed. 61 (2022) e202115024.
[59] D.A. Kleinman, Phys. Rev. 126 (1962) 1977–1979.
[60] C. Aversa, J.E. Sipe, Phys. Rev. B 52 (1995) 14636–14645.
[61] S.N. Rashkeev, W.R.L. Lambrecht, B. Segall, Phys. Rev. B 57 (1998) 3905–3919.